I&EC research
Industrial & Engineering Chemistry Research

Article

Cite This: Ind. Eng. Chem. Res. 2019, 58, 5397−5403

pubs.acs.org/IECR

SSZ-13 Synthesized by Solvent-Free Method: A Potential Candidate for NH_3-SCR Catalyst with High Activity and Hydrothermal Stability

Yulong Shan,[†,‡] Xiaoyan Shi,[†,‡] Jinpeng Du,[†,‡] Zidi Yan,[†,‡] Yunbo Yu,[†,‡,§] and Hong He*[,†,‡,§]

[†]State Key Joint Laboratory of Environment Simulation and Pollution Control, Research Center for Eco-Environmental Sciences, Chinese Academy of Sciences, Beijing, 100085, China

[‡]University of Chinese Academy of Sciences, Beijing 100049, China

[§]Center for Excellence in Regional Atmospheric Environment, Institute of Urban Environment, Chinese Academy of Sciences, Xiamen 361021, China

Supporting Information

ABSTRACT: Seeds were utilized to synthesize high crystallinity and an economical SSZ-13 substrate zeolite with relatively high Si/Al ratio (~11) via a solvent-free method. NH_3-SCR tests, hydrothermal stability, and many characterizations such as XRD, ^{27}Al-NMR, EPR, H_2-TPR, and XAFS were conducted over the fresh and hydrothermally aged Cu^{2+} ion-exchanged zeolite catalysts (Cu-SSZ-13). The fresh catalysts showed high deNOx activity and tolerance to high space velocity in the temperature range from 150 to 550 °C. The active Cu^{2+} ions were hydrothermally stable, resulting in only slight decrease after hydrothermal aging at 800 °C for 16 h. The results showed that the Cu ion-exchanged SSZ-13 catalyst synthesized by the solvent-free method is a promising alternative candidate for actual implementation in diesel engines.

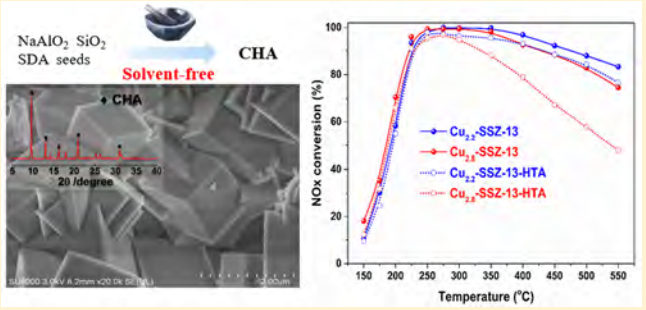

1. INTRODUCTION

Recently, Cu^{2+} ion-exchanged SSZ-13 (Cu-SSZ-13), a zeolite with the chabazite (CHA) structure, has received much attention because of its higher deNOx activity and better hydrothermal stability in comparison to other catalysts.[1,2] In the past few years, there have been extensive studies on the Cu-SSZ-13 catalyst regarding the reaction mechanism,[3−8] determination of active sites,[9−14] hydrothermal stability,[1,15−18] and synthetic method.[19−22] Among these factors, hydrothermal stability should be especially valued because the presence of moisture in the exhaust from DPF regeneration could significantly damage the zeolite framework structure and lead to NOx activity loss for Cu-SSZ-13 catalysts.[1,17] Many studies have proved that dealumination of zeolites and the formation of CuOx clusters from the accumulation of Cu^{2+} species were the primary reasons for the deactivation of Cu-SSZ-13 catalysts during the process of hydrothermal aging.[1,17,23] Therefore, the Si/Al ratio and the Cu^{2+} species were found to be significantly important factors enhancing the hydrothermal stability of Cu-SSZ-13 catalysts. In fact, the dealumination process that typically occurs during hydrothermal aging was inhibited for Cu-SSZ-13 catalysts because the constricting dimensions of the special small-pores limited the detachment of aluminum hydroxide.[24,25] However, despite this advantage, this catalyst always lost its NOx activity when hydrothermally aged at high temperatures.[1,15,17,26] Therefore, solutions must be found to resolve the problem of hydrothermal stability for Cu-SSZ-13 zeolite catalysts.

The traditional method of synthesizing Cu-SSZ-13 zeolite was first reported by Zones in 1985.[27] Nevertheless, the wide application of this catalyst was limited due to the requirement of a very expensive structure-directing agent, *N*,*N*,*N*-trimethyl-1-adamantammonium hydroxide (TMAdaOH), and relatively low yield. The initial Na-SSZ-13 must also be ion-exchanged by NH_4NO_3 and Cu^{2+} salt solutions to obtain Cu-SSZ-13 catalysts. Hence, considering the complexity of ion exchange, Ren et al. developed a one-pot synthetic method of Cu-SSZ-13 catalysts by the use of the economical template copper-tetraethylenepentamine (Cu-TEPA).[19] Then, our group improved this method to obtain high crystallinity Cu-SSZ-13 by decreasing the amount of template required and changing some postprocessing steps.[16,28] The one-pot synthesized Cu-SSZ-13 catalysts showed outstanding NO conversion activity and N_2 selectivity. However, the Si/Al ratio of one-pot synthesized Cu-SSZ-13, at ~4.1, was much lower than optimal, which led to the limited hydrothermal stability of these catalysts. In addition, Corma et al. used Cu-TEPA and TMAdaOH as cooperative organic structure-directing agents (OSDA) to obtain "one-pot" Cu-SSZ-13 zeolites.[29] The synthesized Cu-SSZ-13 sample with Si/Al of 14.2 and Cu/(Si + Al) of 0.059 also showed an obvious decrease in

Received: November 22, 2018
Revised: March 13, 2019
Accepted: March 22, 2019
Published: March 22, 2019

Downloaded by RESEARCH CTR ECO-ENVIRONMENTAL SCI at 02:46:03:895 on June 25, 2019
from https://pubs.acs.org/doi/10.1021/acs.iecr.8b05822.

ACS Publications © 2019 American Chemical Society

DOI: 10.1021/acs.iecr.8b05822
Ind. Eng. Chem. Res. 2019, 58, 5397−5403

performance after being subjected to steam at 750 °C for 13 h. There have been also many other methods reported for synthesizing the Cu-SSZ-13 catalysts with economical templates such as choline chloride, TEA, DMCHABr, or even without a template.[20−22,30]

Among these methods, Wang et al. reported a solvent-free route for synthesizing a relatively high-silica CHA zeolite (Si/Al > 8) by using an economical organic template, *N,N,N*-dimethylethylcyclohexylammonium bromide (DMCHABr).[22] This synthetic strategy was also an environmentally friendly method due to the absence of wastewater as well as high yields. The Cu−S−CHA (Si/Al ∼ 10.5) catalyst exhibited good activity for NO conversion (GHSV = 80 000 h^{-1}). However, the catalytic performance of the solvent-free synthesized Cu-CHA in the SCR reaction was not studied in detail. Considering the hydrothermal stability and economical nature of Cu-SSZ-13 catalysts, the solvent-free synthesis method is a promising route to a practical catalyst for diesel engine exhaust systems. In this study, H-SSZ-13 seeds were used to increase the degree of crystallinity of Na-SSZ-13 zeolite with high Si/Al ratio (Si/Al ∼ 11) synthesized by the solvent-free method. Then, Cu-SSZ-13 samples with different Cu loadings were obtained by ion-exchange procedures with the optimized Na-SSZ-13. The catalytic performance of the synthesized Cu-SSZ-13 in the NH_3-SCR reaction was investigated under different conditions.

2. EXPERIMENTAL SECTION

2.1. Catalyst Synthesis. The initial Na-SSZ-13 was synthesized via a solvent-free route according to Wang et al.[22] In the current study, the solid raw materials were adjusted and composed of Na_2O/SiO_2 (0.22), Si/Al (11.7), DMCHABr/SiO_2 (0.14), and *x* wt % H-SSZ-13 (*x* = 0, 0.1, 1.0, 5, 10%), which was added as seeds. The mixture was finely ground in a mortar and then transferred to an autoclave with a Teflon liner. After heating at 180 °C for 5 days, the sample was completely crystallized. The Na-SSZ-13 was finally obtained by filtration at room temperature and calcination at 600 °C for 6 h. In order to obtain NH_4-SSZ-13, Na-SSZ-13 was ion-exchanged with 1 M NH_4NO_3 solution at 80 °C for 5 h and then filtered and heated at 100 °C for 12 h. Cu-SSZ-13 was obtained by stirring the NH_4-SSZ-13 and a 0.1 M $Cu(NO_3)_2$ solution at ambient temperature for 24 h. High Cu loadings were achieved by repeating the ion exchange process. The final samples were calcined at 600 °C for 6 h. The Si/Al and Cu loadings are shown in Table 1.

The H-SSZ-13 seeds were made based on previous studies.[27] In detail, the gel composition of Na-SSZ-13 was 8.54 g of silica sol (30%), 1.65 g of NaOH, 27.6 g of H_2O, 1 g of NH_4Y, and 4.2 g of TMAdaOH. After stirring well, the solution was transferred into an autoclave and heated at 140 °C for 6 days.

Table 1. Properties of the Na-SSZ-13 and Cu-SSZ-13 Catalysts

sample	Cu contents (wt %)[a]	Si/Al[a]	Cu/Al[a]	micropore areas (m^2/g)[b]	micropore volumes (cm^3/g)[b]
Na-SSZ-13	0	10.9	0	527	0.24
$Cu_{2.2}$-SSZ-13	2.2	10.5	0.25	587	0.22
$Cu_{2.8}$-SSZ-13	2.8	10.4	0.31	512	0.23

[a]Elements were measured by ICP-AES. [b]Micropore area and volume were calculated by t-plot method.

Before ion exchange, the as-synthesized Na-SSZ-13 was calcined in air at 600 °C for 6 h for template removal. The H-SSZ-13 was obtained by calcination of NH_4-SSZ-13, which was made by ion exchange of Na-SSZ-13 with NH_4NO_3 solution.

2.2. NH_3-SCR Activity Test. A fixed-bed quartz flow reactor was used for the SCR activity tests of the sieved powdered catalysts at atmospheric pressure. The composition of reactive gases was as follows: 500 ppm of NO, 500 ppm of NH_3, 5 vol % O_2, 5 vol % H_2O, 25 and 100 ppm of SO_2 (when used), N_2 as balance gas, and total flow rate of 500 mL/min. About 50 mg samples of the catalysts (40−60 mesh size) were tested with a gas hourly space velocity (GHSV) of 400 000 h^{-1}, and different GHSVs were achieved by changing the weight of catalyst. An online Nicolet Is10 spectrometer, which is equipped with a heated, low-volume (0.2 L) multiple-path gas cell (2 m), was used to continuously analyze the effluent gases including NO, NH_3, NO_2, and N_2O. When the test reaction was in a steady state, FTIR spectra were recorded throughout. The NO conversion was calculated according to the following equation:

$$\text{NOx conversion} = \left(1 - \frac{[\text{NOx}]_{\text{out}}}{[\text{NOx}]_{\text{in}}}\right) \times 100\%$$

$$(\text{NOx} = \text{NO} + \text{NO}_2)$$

For the hydrothermal stability tests, about 300 mg (40−60 mesh size) samples of the catalysts were hydrothermally aged (HTA) at 800 °C for 16 h in a 10 vol % H_2O/air feed with a total flow rate of 300 mL/min.

2.3. Catalyst Characterization. The Cu contents and Si/Al ratios of the samples were obtained by using an inductively coupled plasma Atomic Emission Spectrometer (ICP-AES, OPTIMA 2000DV) with a radial view of the plasma. Strong acid solution was used to dissolve the samples before testing. The Cu contents and Si/Al ratios are shown in Table 1. The surface morphology of the zeolites was obtained using field-emission scanning electron microscopy (FE-SEM, SU-8020). N_2 adsorption−desorption isotherms of the samples were measured using a Micromeritics ASAP 2020 system to obtain the micropore areas and pore volumes. Before the N_2 physical adsorption, the catalysts were pretreated at 300 °C for 5 h. Micropore areas and volumes were determined by the t-plot method. Powder X-ray diffraction (PXRD) measurements were carried out at ambient temperature on a computerized Bruker D8 Advance diffractometer with Cu Kα (λ = 0.15406 nm) radiation. The data of 2θ from 5 to 40° were collected using the step size of 0.02°. The solid-state ^{27}Al MAS NMR spectra were collected on a Bruker AVANCE III 400 WB spectrometer using a 4 mm standard bore CP MAS probe. A total of 1000 scans were recorded with 2 s recycle delay for each sample. All ^{27}Al MAS NMR chemical shifts are referenced to the resonances of an aluminum oxide (Al_2O_3) standard (*d* = 11.5).

The electron paramagnetic resonance (EPR) of the samples was recorded at 153 K on a Bruker E500 X-band spectrometer. All catalysts were placed into quartz tubes for the measurement. The tested samples were untreated and exposed to hydrated ambient conditions, in which case all the existing Cu^{2+} active species could be identified. Temperature-programmed reduction with hydrogen (H_2-TPR) experiments were conducted on a Micromeritics AutoChem 2920 chemisorption analyzer. First, ∼0.05 g samples were pretreated

DOI: 10.1021/acs.iecr.8b05822
Ind. Eng. Chem. Res. 2019, 58, 5397−5403

in air (50 mL/min) and cooled down to 50 °C. Then, TCD signal was recorded with the temperature ramping linearly from 50 to 1000 °C at a rate of 10 °C/min in 10% H_2/Ar gas flow (50 mL/min).

X-ray absorption fine structure (XAFS) measurements were conducted at the BL14W1 beamline of the Shanghai Synchrotron Radiation Facility (SSRF). A spectral range of −200 to 800 eV from the Cu K-absorption edge (8979 eV) was collected at ambient conditions in the transmission mode with a Si(111) monochromator. CuO and Cu_2O were used as reference compounds. The background correction, normalization, and linear combination analysis (LCA) of X-ray absorption near-edge structure (XANES) and analysis of extended X-ray absorption fine structure (EXAFS) were analyzed according to the standard procedures using the Athena module implemented in the IFFEFIT software package.[31] The filtered k^2-weighted $\chi(k)$ was Fourier-transformed into R space (k range 3−12.4 Å^{-1}).

3. RESULTS AND DISCUSSION

3.1. Characteristics of Solvent-Free Synthesized Cu-SSZ-13 Catalysts. As many studies have reported,[21,32,33] seeds can direct the synthesis of zeolites and increase the degree of crystallinity of zeolite crystals. Figure 1 exhibits the

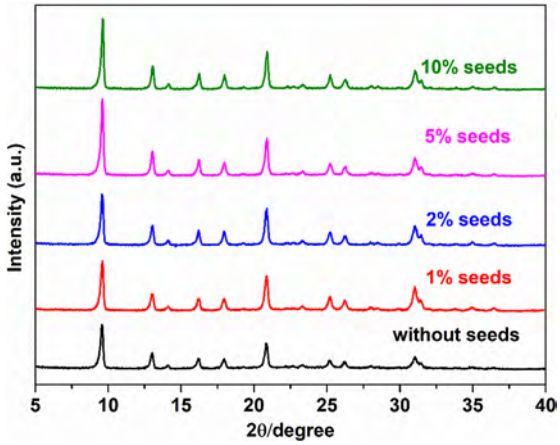

Figure 1. XRD patterns of solvent-free method Na-SSZ-13 with varying seed contents after calcination.

XRD patterns of solvent-free method as-synthesized SSZ-13 prepared with varying seed contents. It is seen that the CHA phase was observed despite the absence of seeds, while the addition of seeds from 1 to 10 wt % increased the intensity of the typical diffraction peaks of CHA zeolite. There was no obvious change in the peak intensities when increasing the seeds from 5 to 10 wt %. Therefore, addition of 5 wt % seeds was sufficient to obtain high crystallinity for the parent SSZ-13 and selected for ion exchange to obtain Cu-SSZ-13 zeolite catalysts. The SEM image (Figure S1) of the Na-SSZ-13 zeolite synthesized by the solvent-free method with the assistance of 5 wt % seeds exhibited a very regular cubic morphology, with particle sizes of 1−2 μm. Figure S2 depicts the N_2 adsorption−desorption isotherms of the Na-SSZ-13 zeolite and its Cu ion-exchanged catalysts (Cu-SSZ-13). All samples showed a type of curve typical of microporous materials, and the micropore areas and volumes of the samples are listed in Table 1.

3.2. NH_3-SCR Performance. Figure 2 shows the NOx conversion as a function of temperature between 150 and 550

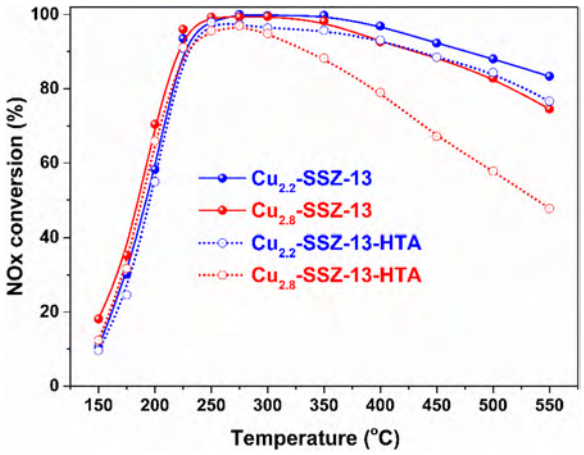

Figure 2. NOx conversion in the NH_3-SCR reaction over the fresh and hydrothermally aged Cu-SSZ-13 catalysts with different Cu loadings. Test conditions: 500 ppm of NO, 500 ppm of NH_3, 5% H_2O, 5% O_2, and N_2 balance. (GHSV = 400 000 h^{-1}).

°C over $Cu_{2.2}$-SSZ-13 and $Cu_{2.8}$-SSZ-13 catalysts. The $Cu_{1.7}$-SSZ-13 catalyst with low Cu loadings was also tested as shown in Figure S3, while it showed low NOx conversion. Both $Cu_{2.2}$-SSZ-13 and $Cu_{2.8}$-SSZ-13 showed outstanding NH_3-SCR performance and reached higher than 80% NO reduction efficiency between 225 and 500 °C with the GHSV of 400 000 h^{-1}. As Cu contents were increased from 2.2 to 2.8 wt %, NO conversion was clearly improved at low temperatures (<250 °C), which demonstrated that the Cu species were the primary active sites. On the contrary, NO reduction activity slightly decreased with additional Cu loading at high temperatures (>400 °C). As mentioned in many studies,[34,35] nonselective NH_3 oxidation by O_2 at high temperatures becomes more dominant with increasing Cu loading. Figure S4 shows the NH_3 conversion of Cu-SSZ-13 catalyst samples. The NH_3 conversion showed the same trend as NO conversion at low temperatures. However, the NH_3 oxidation activity reached 100% at 250 °C and remained at that level until the temperature was 550 °C, while the NO conversion began to decrease at 400 °C, as shown in Figure 2. This demonstrated that there was excessive NH_3 oxidation by O_2 to NOx instead of N_2. Both the catalysts showed excellent selectivity with N_2O production less than 10 ppm at the whole temperature (Figure S5).

In addition, the stable NO reduction activities of $Cu_{2.2}$-SSZ-13 and $Cu_{2.8}$-SSZ-13 catalyst are also illustrated in Figure S6 at temperatures in the range of 150−550 °C with GHSVs of 200 000−800 000 h^{-1}. Both the tested samples showed very high NO conversion, exceeding 80% in a wide operating temperature window between 250 and 500 °C under all GHSV conditions, even at an exceedingly high GHSV of 800 000 h^{-1}, which suggests a high tolerance to severe space velocity conditions. This outstanding characteristic makes it possible to reduce the catalyst installation space on real diesel vehicle SCR after-treatment systems. Considering the presence of SO_2 in practical combustion exhaust, SO_2 was introduced into the standard SCR gas feed, and the SCR reaction activity of $Cu_{2.2}$-SSZ-13 catalyst was evaluated over a wide temperature range of 150−550 °C (as shown in Figure S7). It was observed that

DOI: 10.1021/acs.iecr.8b05822
Ind. Eng. Chem. Res. 2019, 58, 5397−5403

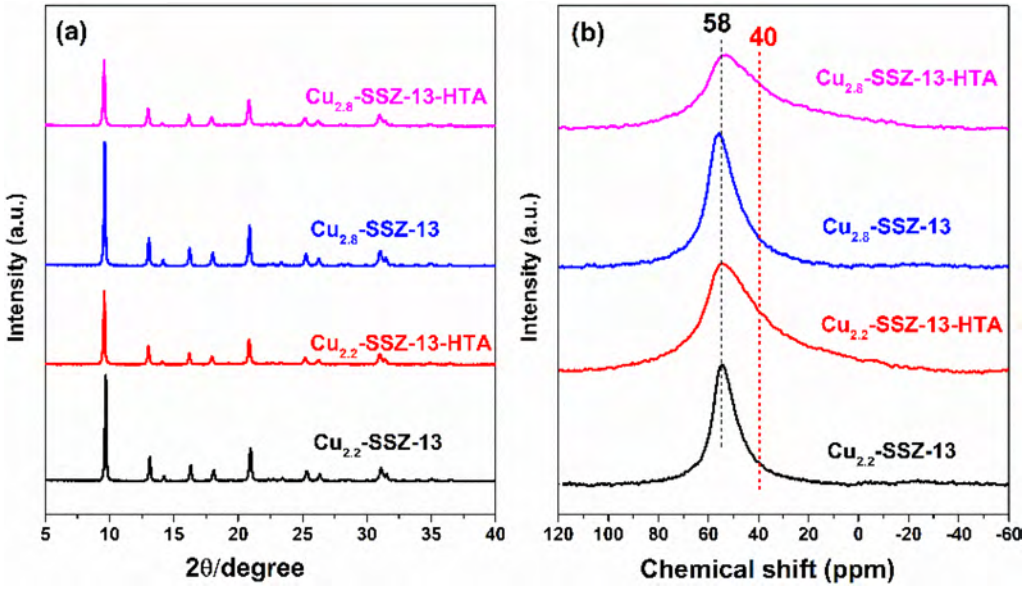

Figure 3. XRD (a) and ^{27}Al-NMR (b) profiles of Cu-SSZ-13 catalysts before and after hydrothermal aging.

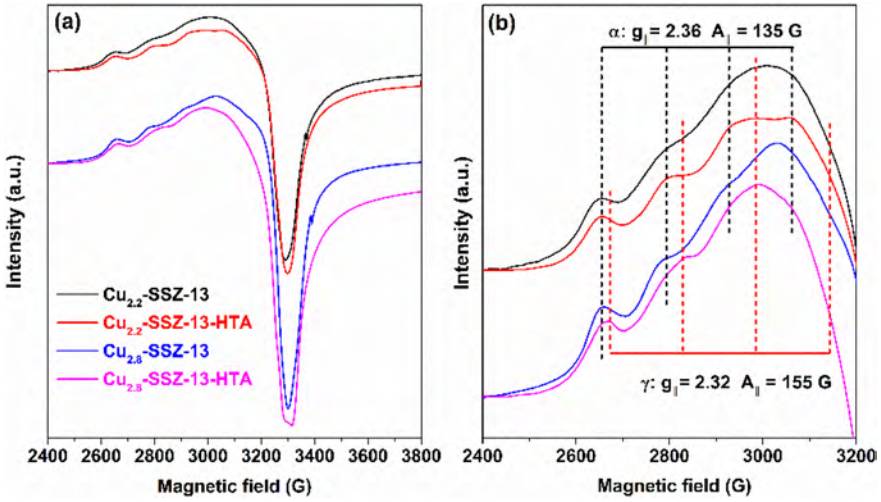

Figure 4. EPR profiles (a) and its magnification (b) of $Cu_{2.2}$-SSZ-13 and $Cu_{2.8}$-SSZ-13 before and after hydrothermal aging.

the NO conversion significantly decreased at low temperatures below 350 °C, while there was no change of NO conversion activity when the temperature was above 350 °C. The tested samples were regenerated in air at 600 °C for 1 h and re-evaluated, and the low-temperature activity was recovered. Therefore, ammonium sulfate like species accumulated and blocked the pore openings at low temperatures, limiting the low-temperature activity,[36] and elevated temperature caused the ammonium sulfate like species to decompose, so the activity was regenerated.[37]

3.3. Hydrothermal Stability. It has been generally known that soot removal by the DPF would lead to SCR catalysts being deactivated when periodically exposed to moisture in the exhaust at high temperatures. Therefore, the NO conversion activity of Cu-SSZ-13 synthesized by solvent-free method was tested after hydrothermal aging with 10 vol % H_2O at 800 °C for 16 h, which is comparable to the exposure of a 135,000 mile vehicle-aged catalyst.[17] As shown in Figure 2, the $Cu_{2.2}$-SSZ-13 catalyst showed a slight decrease of NOx conversion after hydrothermal aging, while higher than 80% of NO conversion was still observed, indicating an outstanding hydrothermal stability. However, the hydrothermally aged $Cu_{2.8}$-SSZ-13 catalyst showed a significant decrease especially at high temperatures (>300 °C) due to the unselective oxidation of NH_3 (Figure S4). Both the hydrothermally aged catalysts showed excellent N_2 selectivity with less than 15 ppm of N_2O production (Figure S5) despite hydrothermal aging at 800 °C.

Figure 3 shows the changes of the zeolite framework structure after hydrothermal aging via XRD and ^{27}Al-NMR measurements. As shown in Figure 3a, both catalysts showed a slight decrease in XRD peak intensity after hydrothermal aging while the zeolite structures with typical CHA peaks remained regardless of the different Cu loadings. In the ^{27}Al-NMR results (Figure 3b), the fresh catalysts showed a prominent peak at ~58 ppm, which is assigned to tetrahedral aluminum incorporated into the framework.[38,39] A signal for extra-framework Al at ~0 ppm chemical shift was not observed, indicating that the fresh catalysts had good crystallinity, which is consistent with the XRD results. After hydrothermal aging at

DOI: 10.1021/acs.iecr.8b05822
Ind. Eng. Chem. Res. 2019, 58, 5397−5403

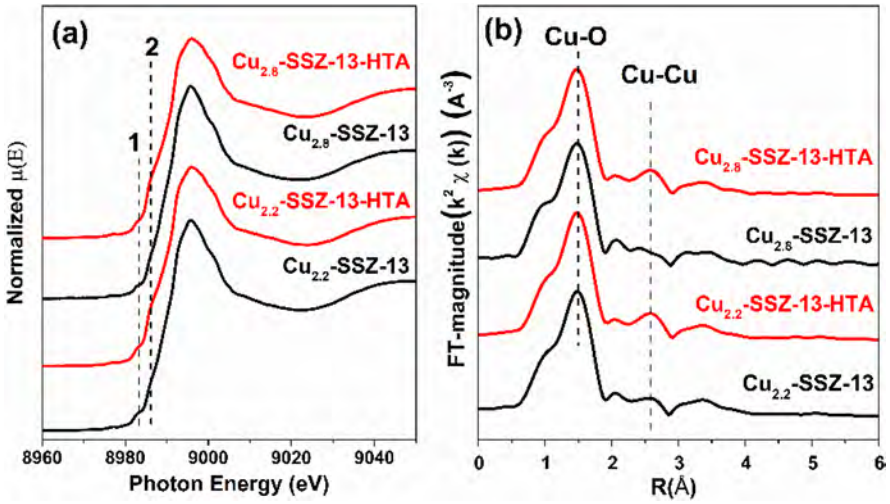

Figure 5. Cu K-edge XANES spectra (a) and k^2-weighted EXAFS spectra (b) of the solvent-free synthesized and commercial Cu-SSZ-13 catalysts.

800 °C for 16 h, the intensity of the peak at 58 ppm decreased to a degree whereas the tetrahedral Al still remained for the most part, which is consistent with the persistent long-range order structure reflected in the XRD profiles. However, after hydrothermal aging, no peak at 0 ppm was observed because of the strong interaction between paramagnetic Cu ions and the formation of octahedral Al.[23] In addition, the hydrothermal aging resulted in the broadening of peaks, which meant that other Al species were formed. The shoulder peak at about 40 ppm can be ascribed to pentahedral Al, a partially framework-bonded Al species.[38,40] From the viewpoint of peak intensity change, it was found that $Cu_{2.8}$-SSZ-13 experienced more dealumination than $Cu_{2.2}$-SSZ-13, which is attributed to much greater CuOx formation in the former case that caused destruction of the zeolite structure.[41]

Electron paramagnetic resonance (EPR) is an effective characterization technique to verify the Cu^{2+} species composition, because only Cu^{2+} (or $Cu(H_2O)_6^{2+}$) is EPR active, while CuOx (or Cu^+) clusters are EPR silent.[8,41] In this case, by distinguishing the change in the EPR signal after hydrothermal aging, the transformation of Cu^{2+} to CuOx could be estimated. Figure 4 depicts the EPR profiles, which were collected at 155 K in order to avoid the broadening effect due to the Cu^{2+} species mobility. Clearly, the EPR signal of the Cu^{2+} species peak decreased after hydrothermal aging for both the Cu-SSZ-13 catalysts, indicating that CuOx clusters formed. To further precisely observe the Cu^{2+} species, the hyperfine peaks at low magnetic field were magnified and shown in Figure 4b. It can be seen that there is only one spectra feature (α: $g_{\|}$ = 2.36 and $A_{\|}$ = 135 G), which was ascribed to the active Cu^{2+} ions in the NH_3-SCR reaction.[1,8] However, after hydrothermal aging, a new species (γ: $g_{\|}$ = 2.32 and $A_{\|}$ = 155 G) appeared especially on the hydrothermally aged $Cu_{2.8}$-SSZ-13-HTA, which is ascribed to Cu^{2+}-Al_2O_3.[1] This indicated that the extra-framework Al formed (also can be seen in Figure 3b) and is coordinated to Cu^{2+}, therefore deactivating the deNOx efficiency.

XAFS measurement was further carried out to determine the state of Cu species of the fresh and hydrothermally aged Cu-SSZ-13 catalysts. As shown in Figure 5a, compared to fresh catalysts, the hydrothermally aged Cu-SSZ-13 catalysts showed two additional features, which were ascribed to the 1s → $4p_{xy}$ electronic transition on 2-coordinate Cu^+ (Figure S8, Cu_2O, ~8982 eV) and 1s → $4p_z$ electronic transition on 4-coordinate Cu^{2+} (Figure S8, CuO, ~8986 eV).[1,11,42] Linear combination analysis (LCA) was carried out to further quantify the amounts of different Cu species, the result of which is shown in Table 2.

Table 2. Distribution of Cu Species by Linear Combination Fit Analysis of XANES Spectra

samples	Cu^{2+} (%)[a]	Cu_2O (%)	CuO (%)
$Cu_{2.2}$-SSZ-13	100	0	0
$Cu_{2.2}$-SSZ-13-HTA	83.3	4	12.6
$Cu_{2.8}$-SSZ-13	100	0	0
$Cu_{2.8}$-SSZ-13-HTA	82.4	5.3	12.3

[a]Cu_2O and CuO were employed as standard copper compounds, and the XANES spectra of $Cu_{2.2}$-SSZ-13 was employed as a reference for the Cu^{2+} ions.

It was clearly seen that the hydrothermally aged $Cu_{2.8}$-SSZ-13 showed more CuOx formation (17.6%), consistent with the results of EPR analyses. Meanwhile, EXAFS was also conducted to identify the different Cu shells. As depicted in Figure 5b, the Cu−Cu bond peaks become stronger for the hydrothermally aged Cu-SSZ-13 catalyst, especially the $Cu_{2.8}$-SSZ-13 catalyst, indicating the formation of CuOx.

Moreover, we conducted H_2-TPR measurement to identify the different Cu species, which was presented in Figure 6. According to previous studies, the Cu^{2+} species reduction occurred in two steps, which included the reduction of Cu^{2+} to Cu^+ (<500 °C) and Cu^+ to Cu^0 (>500 °C).[1,8,16] The Cu-SSZ-13 catalysts also contain two kinds of Cu^{2+} species: isolated Cu^{2+} (Cu^{2+}-2Z) in D6R cages balanced with two framework negative charges and $[Cu(OH)]^+$-Z in CHA cages balanced with one negative charge.[41,43] To quantitatively calculate the relative amounts of different Cu^{2+} species, the reduction peak was deconvoluted, after which the peak could be well-attributed to the different Cu^{2+} species. The peaks at ~200 °C and ~375 °C were attributed to the reduction of $[Cu(OH)]^+$-Z species in CHA cages and Cu^{2+}-2Z species in D6R cages, respectively. The peaks at ~250 °C represented CuO species. The high-temperature peak (>500 °C) was resulted from the reduction of Cu^+ to Cu^0. The relative ratios of Cu^{2+}-2Z and $Cu(OH)^+$-Z species are listed in Table 3, based on the intensities of the reduction peaks. The CuOx peak,

DOI: 10.1021/acs.iecr.8b05822
Ind. Eng. Chem. Res. 2019, 58, 5397−5403

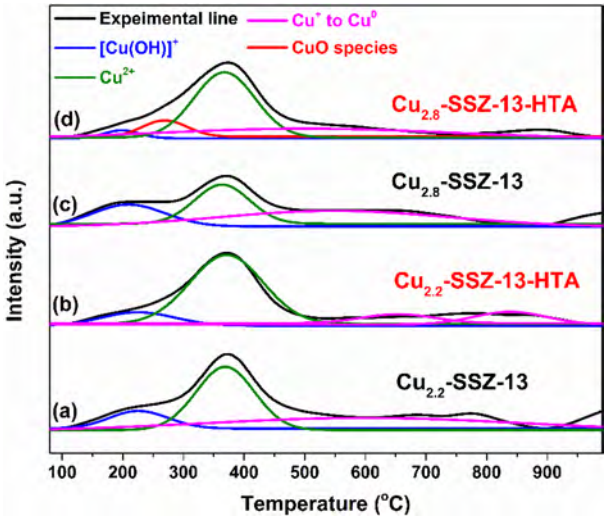

Figure 6. H_2-TPR profiles of solvent-free synthesized and commercial Cu-SSZ-13 catalysts before and after hydrothermal aging.

Table 3. Distribution and Contents of Cu^{2+} Species Based on TPR Analysis

samples	$[Cu(OH)]^+$-Z (%)	Cu^{2+}-2Z (%)	CuOx (%)
$Cu_{2.2}$-SSZ-13	22	78	0
$Cu_{2.2}$-SSZ-13-HTA	16	84	0
$Cu_{2.8}$-SSZ-13	43	57	0
$Cu_{2.8}$-SSZ-13-HTA	6	80	14

which has been identified by EPR and XAFS, was not observed over $Cu_{2.2}$-SSZ-13-HTA, probably due to very few CuOx formation covered easily by the H_2 consumption peak of Cu^{2+} species. However, it is worth noting that the proportion of Cu^{2+}-2Z increased from 78 to 84%, accompanied by the decrease of $[Cu(OH)]^+$-Z from 22 to 16%, indicating the conversion of $[Cu(OH)]^+$-Z to Cu^{2+}-2Z, which has been also reported by Song et al.[41] This process resulted in a decrease of NOx conversion, because Cu^{2+}-2Z is less active than $[Cu(OH)]^+$-Z. In the case of $Cu_{2.8}$-SSZ-13, however, CuOx formation occurred although the Cu^{2+}-2Z species increased from 57 to 80% after hydrothermal aging. All the characterization results indicated that the Cu-exchanged SSZ-13 synthesized by the solvent-free method has excellent hydrothermal stability due to the stable zeolite structure or active Cu^{2+} species.

4. CONCLUSIONS

SSZ-13 zeolite with relatively high crystallinity and Si/Al ratio (~11) was synthesized by the solvent-free method with the addition of seeds. The Cu ion-exchanged SSZ-13 showed excellent NH_3-SCR activity under different conditions and good resistance to SO_2. Moreover, based on the Si/Al of ~11, the $Cu_{2.2}$-SSZ-13 with Cu loading of 2.2 wt % and Cu/Al of 0.25 maintained its excellent deNOx efficiency even after hydrothermal aging at 800 °C for 16 h, indicating an outstanding hydrothermal stability. Therefore, the solvent-free synthetic method is an optimal candidate for preparing Cu-SSZ-13 catalysts with high NH_3-SCR activity and hydrothermal stability.

■ ASSOCIATED CONTENT

Supporting Information

The Supporting Information is available free of charge on the ACS Publications website at DOI: 10.1021/acs.iecr.8b05822.

N_2 adsorption−desorption isotherms, NO and NH_3 conversion and N_2O production of Cu-SSZ-13 with different Cu loadings, XRD profiles for the commercial Cu-SSZ-13 catalysts before and after hydrothermal aging (PDF)

■ AUTHOR INFORMATION

Corresponding Author

*Tel.: +86 10 62849123. Fax: +86 10 62849123. E-mail: honghe@rcees.ac.cn.

ORCID

Yulong Shan: 0000-0002-5031-8522

Yunbo Yu: 0000-0003-2935-0955

Notes

The authors declare no competing financial interest.

■ ACKNOWLEDGMENTS

This work was financially supported by the National Natural Science Foundation of China (21637005, 51578536, and 21777174).

■ REFERENCES

(1) Kim, Y. J.; Lee, J. K.; Min, K. M.; Hong, S. B.; Nam, I.-S.; Cho, B. K. Hydrothermal stability of CuSSZ13 for reducing NOx by NH_3. *J. Catal.* **2014**, *311*, 447−457.

(2) Kwak, J. H.; Tonkyn, R. G.; Kim, D. H.; Szanyi, J.; Peden, C. H. F. Excellent activity and selectivity of Cu-SSZ-13 in the selective catalytic reduction of NOx with NH_3. *J. Catal.* **2010**, *275* (2), 187−190.

(3) Kwak, J. H.; Lee, J. H.; Burton, S. D.; Lipton, A. S.; Peden, C. H.; Szanyi, J. A common intermediate for N_2 formation in enzymes and zeolites: side-on Cu-nitrosyl complexes. *Angew. Chem.* **2013**, *125* (38), 10169−10173.

(4) Xie, L.; Liu, F.; Liu, K.; Shi, X.; He, H. Inhibitory effect of NO_2 on the selective catalytic reduction of NOx with NH_3 over one-pot-synthesized Cu-SSZ-13 catalyst. *Catal. Sci. Technol.* **2014**, *4* (4), 1104−1110.

(5) Su, W.; Chang, H.; Peng, Y.; Zhang, C.; Li, J. Reaction pathway investigation on the selective catalytic reduction of NO with NH_3 over Cu/SSZ-13 at low temperatures. *Environ. Sci. Technol.* **2015**, *49* (1), 467−473.

(6) Lomachenko, K. A.; Borfecchia, E.; Negri, C.; Berlier, G.; Lamberti, C.; Beato, P.; Falsig, H.; Bordiga, S. The Cu-CHA deNOx Catalyst in Action: Temperature-Dependent NH_3-Assisted Selective Catalytic Reduction Monitored by Operando XAS and XES. *J. Am. Chem. Soc.* **2016**, *138* (37), 12025−8.

(7) Paolucci, C.; Parekh, A. A.; Khurana, I.; Di Iorio, J. R.; Li, H.; Albarracin Caballero, J. D.; Shih, A. J.; Anggara, T.; Delgass, W. N.; Miller, J. T.; Ribeiro, F. H.; Gounder, R.; Schneider, W. F. Catalysis in a Cage: Condition-Dependent Speciation and Dynamics of Exchanged Cu Cations in SSZ-13 Zeolites. *J. Am. Chem. Soc.* **2016**, *138* (18), 6028−48.

(8) Gao, F.; Walter, E. D.; Karp, E. M.; Luo, J.; Tonkyn, R. G.; Kwak, J. H.; Szanyi, J.; Peden, C. H. F. Structure−activity relationships in NH_3-SCR over Cu-SSZ-13 as probed by reaction kinetics and EPR studies. *J. Catal.* **2013**, *300*, 20−29.

(9) Zhu, H.; Kwak, J. H.; Peden, C. H. F.; Szanyi, J. In situ DRIFTS-MS studies on the oxidation of adsorbed NH_3 by NOx over a Cu-SSZ-13 zeolite. *Catal. Today* **2013**, *205*, 16−23.

DOI: 10.1021/acs.iecr.8b05822
Ind. Eng. Chem. Res. 2019, 58, 5397−5403

(10) Hun Kwak, J.; Zhu, H.; Lee, J. H.; Peden, C. H.; Szanyi, J. Two different cationic positions in Cu-SSZ-13? *Chem. Commun.* **2012**, *48* (39), 4758−4760.
(11) Bates, S. A.; Verma, A. A.; Paolucci, C.; Parekh, A. A.; Anggara, T.; Yezerets, A.; Schneider, W. F.; Miller, J. T.; Delgass, W. N.; Ribeiro, F. H. Identification of the active Cu site in standard selective catalytic reduction with ammonia on Cu-SSZ-13. *J. Catal.* **2014**, *312*, 87−97.
(12) Gao, F.; Washton, N. M.; Wang, Y.; Kollár, M.; Szanyi, J.; Peden, C. H. F. Effects of Si/Al ratio on Cu/SSZ-13 NH_3-SCR catalysts: Implications for the active Cu species and the roles of Brønsted acidity. *J. Catal.* **2015**, *331*, 25−38.
(13) Verma, A. A.; Bates, S. A.; Anggara, T.; Paolucci, C.; Parekh, A. A.; Kamasamudram, K.; Yezerets, A.; Miller, J. T.; Delgass, W. N.; Schneider, W. F.; Ribeiro, F. H. NO oxidation: A probe reaction on Cu-SSZ-13. *J. Catal.* **2014**, *312*, 179−190.
(14) Shan, Y.; Shi, X.; He, G.; Liu, K.; Yan, Z.; Yu, Y.; He, H. Effects of NO_2 Addition on the NH_3-SCR over Small-Pore Cu-SSZ-13 Zeolites with Varying Cu Loadings. *J. Phys. Chem. C* **2018**, *122* (45), 25948−25953.
(15) Wang, D.; Jangjou, Y.; Liu, Y.; Sharma, M. K.; Luo, J.; Li, J.; Kamasamudram, K.; Epling, W. S. A comparison of hydrothermal aging effects on NH_3-SCR of NOx over Cu-SSZ-13 and Cu-SAPO-34. *Appl. Catal., B* **2015**, *165*, 438−445.
(16) Xie, L.; Liu, F.; Shi, X.; Xiao, F.-S.; He, H. Effects of post-treatment method and Na co-cation on the hydrothermal stability of Cu-SSZ-13 catalyst for the selective catalytic reduction of NOx with NH_3. *Appl. Catal., B* **2015**, *179*, 206−212.
(17) Schmieg, S. J.; Oh, S. H.; Kim, C. H.; Brown, D. B.; Lee, J. H.; Peden, C. H. F.; Kim, D. H. Thermal durability of Cu-CHA NH_3-SCR catalysts for diesel NOx reduction. *Catal. Today* **2012**, *184* (1), 252−261.
(18) Shan, Y.; Shi, X.; Yan, Z.; Liu, J.; Yu, Y.; He, H. Deactivation of Cu-SSZ-13 in the presence of SO_2 during hydrothermal aging. *Catal. Today* **2019**, *320*, 84−90.
(19) Ren, L.; Zhu, L.; Yang, C.; Chen, Y.; Sun, Q.; Zhang, H.; Li, C.; Nawaz, F.; Meng, X.; Xiao, F. S. Designed copper-amine complex as an efficient template for one-pot synthesis of Cu-SSZ-13 zeolite with excellent activity for selective catalytic reduction of NOx by NH_3. *Chem. Commun.* **2011**, *47* (35), 9789−9791.
(20) Chen, B.; Xu, R.; Zhang, R.; Liu, N. Economical way to synthesize SSZ-13 with abundant ion-exchanged Cu^+ for an extraordinary performance in selective catalytic reduction (SCR) of NOx by ammonia. *Environ. Sci. Technol.* **2014**, *48* (23), 13909−13916.
(21) Zhao, Z.; Yu, R.; Zhao, R.; Shi, C.; Gies, H.; Xiao, F.-S.; De Vos, D.; Yokoi, T.; Bao, X.; Kolb, U.; Feyen, M.; McGuire, R.; Maurer, S.; Moini, A.; Müller, U.; Zhang, W. Cu-exchanged Al-rich SSZ-13 zeolite from organotemplate-free synthesis as NH_3 -SCR catalyst: Effects of Na^+ ions on the activity and hydrothermal stability. *Appl. Catal., B* **2017**, *217*, 421−428.
(22) Wang, X.; Wu, Q.; Chen, C.; Pan, S.; Zhang, W.; Meng, X.; Maurer, S.; Feyen, M.; Muller, U.; Xiao, F. S. Atom-economical synthesis of a high silica CHA zeolite using a solvent-free route. *Chem. Commun.* **2015**, *51* (95), 16920−3.
(23) Kwak, J. H.; Tran, D.; Burton, S. D.; Szanyi, J.; Lee, J. H.; Peden, C. H. F. Effects of hydrothermal aging on NH_3-SCR reaction over Cu/zeolites. *J. Catal.* **2012**, *287*, 203−209.
(24) Fickel, D. W.; D'Addio, E.; Lauterbach, J. A.; Lobo, R. F. The ammonia selective catalytic reduction activity of copper-exchanged small-pore zeolites. *Appl. Catal., B* **2011**, *102* (3−4), 441−448.
(25) Blakeman, P. G.; Burkholder, E. M.; Chen, H.-Y.; Collier, J. E.; Fedeyko, J. M.; Jobson, H.; Rajaram, R. R. The role of pore size on the thermal stability of zeolite supported Cu SCR catalysts. *Catal. Today* **2014**, *231*, 56−63.
(26) Ma, L.; Cheng, Y.; Cavataio, G.; McCabe, R. W.; Fu, L.; Li, J. Characterization of commercial Cu-SSZ-13 and Cu-SAPO-34 catalysts with hydrothermal treatment for NH_3-SCR of NOx in diesel exhaust. *Chem. Eng. J.* **2013**, *225*, 323−330.
(27) Zones, S. I. Conversion of Faujasites to High-silica Chabazite SSZ-13 in the Presence of N,N,N-Trimethyl-1-adamantammonium lodide. *J. Chem. Soc., Faraday Trans.* **1991**, *87*, 3709−3716.
(28) Xie, L.; Liu, F.; Ren, L.; Shi, X.; Xiao, F. S.; He, H. Excellent performance of one-pot synthesized Cu-SSZ-13 catalyst for the selective catalytic reduction of NOx with NH_3. *Environ. Sci. Technol.* **2014**, *48* (1), 566−572.
(29) Martínez-Franco, R.; Moliner, M.; Thogersen, J. R.; Corma, A. Efficient One-Pot Preparation of Cu-SSZ-13 Materials using Cooperative OSDAs for their Catalytic Application in the SCR of NOx. *ChemCatChem* **2013**, *5* (11), 3316−3323.
(30) Martin, N.; Moliner, M.; Corma, A. High yield synthesis of high-silica chabazite by combining the role of zeolite precursors and tetraethylammonium: SCR of NOx. *Chem. Commun.* **2015**, *51* (49), 9965−8.
(31) Newville, M. Interactive XAFS Analysis and FEFF Fitting. *J. Synchrotron Radiat.* **2001**, *8* (8), 322−324.
(32) Imai, H.; Hayashida, N.; Yokoi, T.; Tatsumi, T. Direct crystallization of CHA-type zeolite from amorphous aluminosilicate gel by seed-assisted method in the absence of organic-structure-directing agents. *Microporous Mesoporous Mater.* **2014**, *196*, 341−348.
(33) Ji, Y.; Wang, Y.; Xie, B.; Xiao, F.-S. Zeolite Seeds: Third Type of Structure Directing Agents in the Synthesis of Zeolites. *Comments Inorg. Chem.* **2016**, *36* (1), 1−16.
(34) Kwak, J. H.; Tran, D.; Szanyi, J.; Peden, C. H. F.; Lee, J. H. The Effect of Copper Loading on the Selective Catalytic Reduction of Nitric Oxide by Ammonia Over Cu-SSZ-13. *Catal. Lett.* **2012**, *142* (3), 295−301.
(35) Park, J.; Park, H.; Baik, J.; Nam, I.; Shin, C.; Lee, J.; Cho, B.; Oh, S. Hydrothermal stability of CuZSM5 catalyst in reducing NO by NH_3 for the urea selective catalytic reduction process. *J. Catal.* **2006**, *240* (1), 47−57.
(36) Luo, J.; Wang, D.; Kumar, A.; Li, J.; Kamasamudram, K.; Currier, N.; Yezerets, A. Identification of two types of Cu sites in Cu/SSZ-13 and their unique responses to hydrothermal aging and sulfur poisoning. *Catal. Today* **2016**, *267*, 3−9.
(37) Brookshear, D. W.; Nam, J.-g.; Nguyen, K.; Toops, T. J.; Binder, A. Impact of sulfation and desulfation on NOx reduction using Cu-chabazite SCR catalysts. *Catal. Today* **2015**, *258*, 359−366.
(38) Prodinger, S.; Derewinski, M. A.; Wang, Y.; Washton, N. M.; Walter, E. D.; Szanyi, J.; Gao, F.; Wang, Y.; Peden, C. H. F. Sub-micron Cu/SSZ-13: Synthesis and application as selective catalytic reduction (SCR) catalysts. *Appl. Catal., B* **2017**, *201*, 461−469.
(39) Zhang, T.; Qiu, F.; Li, J. Design and synthesis of core-shell structured meso-Cu-SSZ-13@mesoporous aluminosilicate catalyst for SCR of NOx with NH_3: Enhancement of activity, hydrothermal stability and propene poisoning resistance. *Appl. Catal., B* **2016**, *195*, 48−58.
(40) Haouas, M.; Taulelle, F.; Martineau, C. Recent advances in application of (27)Al NMR spectroscopy to materials science. *Prog. Nucl. Magn. Reson. Spectrosc.* **2016**, *94*−*95*, 11−36.
(41) Song, J.; Wang, Y.; Walter, E. D.; Washton, N. M.; Mei, D.; Kovarik, L.; Engelhard, M. H.; Prodinger, S.; Wang, Y.; Peden, C. H. F.; Gao, F. Toward Rational Design of Cu/SSZ-13 Selective Catalytic Reduction Catalysts: Implications from Atomic-Level Understanding of Hydrothermal Stability. *ACS Catal.* **2017**, *7* (12), 8214−8227.
(42) Lezcano-Gonzalez, I.; Deka, U.; van der Bij, H. E.; Paalanen, P.; Arstad, B.; Weckhuysen, B. M.; Beale, A. M. Chemical deactivation of Cu-SSZ-13 ammonia selective catalytic reduction (NH_3-SCR) systems. *Appl. Catal., B* **2014**, *154*−*155* (0), 339−349.
(43) Jangjou, Y.; Do, Q.; Gu, Y.; Lim, L.-G.; Sun, H.; Wang, D.; Kumar, A.; Li, J.; Grabow, L. C.; Epling, W. On the nature of Cu active centers in Cu-SSZ-13 and their responses to SO_2 exposure. *ACS Catal.* **2018**, *8*, 1325.

DOI: 10.1021/acs.iecr.8b05822
Ind. Eng. Chem. Res. 2019, 58, 5397−5403